

Graph-Cut Based Edge Detection for Kalman Filter Based Left Ventricle Tracking in 3D+T Echocardiography

Engin Dikici¹, Fredrik Orderud²

¹Norwegian University of Science and Technology, Trondheim, Norway

²GE Vingmed Ultrasound, Oslo, Norway

Abstract

Consistent endocardial border segmentation in 3D echocardiography is a challenging task. One of the major difficulties rises due to the fact that the trabeculated structure of the endocardium causes the endocardial intensity profile characteristics to change over a cardiac cycle. In this paper, we present a hybrid edge detection approach using both max flow/min cut (MFMC) and step criterion (STEP) edge detectors, and its integration into a Kalman filter based left ventricle (LV) tracking framework.

We treat the endocardial edge detection problem as a graph partitioning problem where the graph is defined by using the intensity profiles, and propose a max flow/min cut based solution. For the end-systole, the step criterion edge detector is a more suitable option. Accordingly, we introduce the weighted combination of these techniques called the hybrid edge detector (Hybrid) where the weight factor is determined by the size of the tracked endocardial mesh.

Surface and volumetric measurement comparisons between the STEP, MFMC and Hybrid shows that the Hybrid handles the specific problem of time-dependent intensity profiles better than the other approaches.

1. Introduction

The introduction of 3D echocardiography has enabled rapid and low-cost acquisition of volumetric images of the left ventricle (LV). Numerous techniques for segmenting these images have appeared in the literature. However, accurate and consistent detection of the endocardial border still remains a challenging task. Part of the reason for this is that the trabeculated structure of the endocardial boundary leads to alternating edge characteristics over a cardiac cycle.

Kalman filter-based 3D segmentation adopts a sequential prediction and update strategy; the surface deformations are predicted by using a kinematic model, then the prediction is updated based on the information provided by image measurements. Normal displacement measure-

ments, where the object border search is performed on a set of normal lines defined on the predicted surface, are commonly preferred during the measurement process. In an early work by Blake et al., Kalman filtering was used for tracking B-spline models deformed in an affine shape space [1]. In their study, the normal displacements were determined by selecting the gradient maxima of the image intensity profiles. Later, this framework was utilized with a principal component analysis based shape space for LV tracking in 2D ultrasound [2]. A local-phase edge detector [3] was applied for the measurements, and improved results were reported. More recently, a framework that uses extended Kalman filtering for tracking subdivision surfaces in 3D image data sets was introduced by Orderud et al. [4]. In their study, a step criterion was applied for the detection of the edges [5]. Common in all these studies, for a given contour/mesh, the normal displacement for each edge position is found independently from the other edge positions, which does not exploit the relationship between the neighboring intensity profiles.

Given a shape model positioned in a close proximity of the target object border, max flow/min-cut algorithms from the combinatorial optimization can be used for updating the model points closer to their target locations. This may be achieved by processing the graph consisting of the information gathered from a narrow-band around the target object contour. In the graph-cut based active contours study [6], the optimal object contour was located by calculating the minimal cut for a narrow-band graph iteratively. Later, a similar approach was used for the segmentation of elliptical objects [7]. The remainder of this paper illustrates how the max-flow / min-cut algorithm in narrow-band graphs may be utilized for the endocardial border detection.

2. Methods

2.1. Tracking framework

The framework is built around a deformable subdivision model parametrized by a set of control vertices and

their associated displacement direction vectors. Model deformations are handled by a composite transform, where local shape deformations are obtained by moving control vertices in the subdivision model together with a global transformation that translates, rotates and scales the whole model.

A manually constructed Doo-Sabin surface is used to represent the endocardial borders. This model consists of 20 control vertices that are allowed to move in the surface normal direction to alter the shape. The edge detection is conducted from a set of approximately 500 surface points, spread evenly across the endocardial surface.

The tracking framework consists of five separate stages, namely the (1) state prediction, (2) evaluation of tracking model, (3) edge measurements, (4) measurement assimilation, and (5) measurement update. In this study, the stages are identical as in [4], and therefore not covered. The endocardial edge detection performed at the *edge measurements* stage is further investigated.

2.2. Edge detection methods

The edge detection process is performed by first extracting N intensity profiles $I = \{I_i | i \in \{1, \dots, N\}\}$, where each profile is centered around a surface point p_i and oriented in a surface normal direction n_i . The total number of samples in each profile, K , and the distance between consecutive samples are determined empirically. $I_{i,k}$ is used for referring to the intensity value of the i^{th} intensity profile's k^{th} sample ($I_{i, \frac{K}{2}}$ gives the intensity value at p_i). The function L gives the index of the most probable edge in each intensity profile, and is described for different edge detection methods in the following subsections.

2.2.1. Step criterion edge detector (STEP)

STEP assumes that the intensity profile I_i forms a transition from one intensity plateau to another. It calculates the average intensity heights of the two plateaus for each index value, and selects the index with the lowest model-data disagreement. The measurement noise can be set as the inverse of the height difference between the plateaus. For each profile, the edge index is determined as:

$$L_i = \arg \min_{k \in \{0 \dots K-1\}} \left(\sum_{t=0}^k \left| \left(\frac{1}{k+1} \sum_{j=0}^k I_{i,j} \right) - I_{i,t} \right| + \sum_{t=k+1}^{K-1} \left| \left(\frac{1}{K-k-1} \sum_{j=k+1}^K I_{i,j} \right) - I_{i,t} \right| \right). \quad (1)$$

2.2.2. Max flow / min cut edge detector (MFMC)

Max flow/min cut algorithms from combinatorial optimization can be used for finding the global optima of a set of important energy functions [8]. A very common energy function that is addressed by Greig et al. can be expressed as:

$$E(f) = \sum_{v \in V} D_v(f_v) + \sum_{(v,y) \in Edges} Q_{v,y}(f_v, f_y). \quad (2)$$

The optimization process seeks a labeling function f that assigns binary values to the nodes that are defined under a set V , distinguishing the inside of the LV cavity ($f = 1$) from the outside ($f = 0$). The classification is constrained by *data penalty* D_v , and *interaction potential* $Q_{v,y}$ functions. In this setting, (1) D_v penalizes the labeling of v based on the predefined likelihood function, and (2) $Q_{v,y}$ penalizes the labeling discontinues between the neighboring nodes v and y .

The problem of finding the optimal edges for a set of intensity profiles is formulated as in *eqn-2* by the MFMC method. Initially, a graph with nodes corresponding to the each profile sample is created. Two additional terminal nodes, the source and the sink, corresponding to the inside and the outside of the endocardium are appended to the node-set. The source and the sink are connected by edges to the nodes corresponding to the first and the last members of the intensity profiles respectively. The edges connecting the terminals to the other nodes are referred as the *t-links*, and they are set with infinite weights, which guarantees null data penalties in *eqn-2*.

The nodes corresponding to (1) the consecutive samples of the same profile, and (2) the same index samples of the neighboring profiles, are connected by undirected weighted edges called the *n-links*. For the first case, the weight of an n-link that connects nodes v and y can be calculated as:

$$weight(v, y) = C \times \exp \left(\frac{-(I_v - I_y)^2}{2\sigma^2} \right), \quad (3)$$

where I_v and I_y refers to the intensity values at the associated profile samples and C is a constant.

For the second case, when the inter-profile connections are formed, the weight function from *eqn-3* is multiplied with a *smoothness constant*. The smoothness constant ensures that the final cut finds the proximate edge indexes for the neighboring profiles (see figure 1).

After the graph is created, the maximum flow / minimum cut between the source and the sink nodes are found

by the push-relabel algorithm [9] in a polynomial time $O(|V|^3)$. The resulting cut defines the edge positions for all intensity profiles simultaneously. Furthermore, the reverse of the flow is proportional with the quality of the cut, and therefore can be utilized as the measurement noise in the Kalman filter.

2.2.3. Tradeoffs for the sole applications of the edge detectors

Including the trabeculae in the LV volume is a commonly accepted practice for enhancing the reproducibility of the LV measurements [10]. At the end-diastole (ED), the trabeculations are filled with blood, and therefore cause strong intensity changes across the endocardial surface. STEP criteria is prone to including trabeculae with the myocardium, since it processes each intensity profile independently. MFMC, on the other hand, is observed to behave better in this scenario, since the smoothness criteria constrained by the inter-profile n-links leads to more consistent edge indexes. The trabeculations are thus included with the cavity (see figure 2).

At the end-systole (ES), the edge detection problem attains a different form. Due to the compression and folding, the trabeculae appears as a part of the myocardium, making the intensity profiles more continuous. The inter-profile n-links that previously was an advantage for MFMC at ED then turns into a burden. The smoother profiles eliminate the need for them, and they limit the agility of the model when it is most needed. On the other hand, STEP performs well at ES (see figure 2).

2.2.4. Hybrid edge detector

The weighted average of MFMC and STEP edge indexes, a *hybrid* edge index, is computed for each intensity

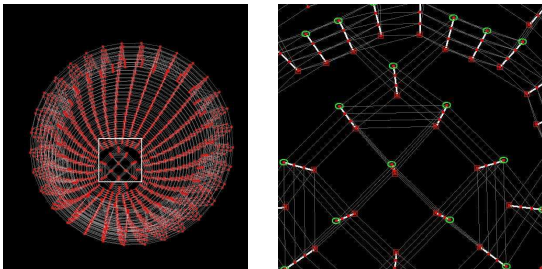


Figure 1. Left: The graph nodes are shown with red, and the n-links with gray. Right: (A closer look at the graph) the graph nodes are shown with red, the nodes having t-links with the source are shown in red boxes, the nodes having t-links with the sink are shown in ellipsoids, the inter-profile n-links are shown with gray, and the in-profile n-links with white.

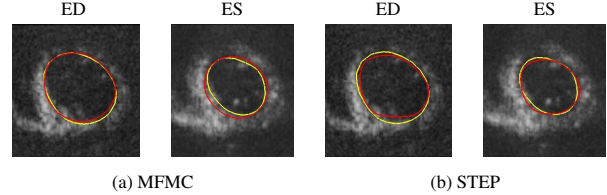


Figure 2. The reference contours are shown with yellow, and the tracker result with red. (a) MFMC edges are fitting well to the reference at ED, there is an over-estimation happening at ES. (b) STEP edges are fitting well to the reference at ES, there is an under-estimation happening at ED.

profile during the cardiac cycle. The weight factor is determined by the size of the endocardial mesh. As the mesh size converges to its maxima, the relative weight for the MFMC increases, and as it converges to its minima, the relative weight for the STEP increases. For each profile, the edge index is determined by finding

$$L_i^{hybrid} = \beta L_i^{MFMC} + (1 - \beta) L_i^{STEP}, \quad (4)$$

where $\beta = (meshsize(t) - meshsize(ES)) / (meshsize(ED) - meshsize(ES))$.

3. Results

A set of 10 apical 3D echocardiography recordings, which includes 3 normal cases and 7 cases from patients with heart diseases, was used for the evaluation. The recordings were acquired using a Vivid 7 ultrasound scanner (GE Vingmed Ultrasound, Norway) using a matrix array transducer. The STEP, MFMC and Hybrid edge detectors were each used in connection to the existing contour tracking framework. Tracked 3D meshes were extracted after running the tracker through 3 cardiac cycles for a convergence. The accuracy of the edge detectors were evaluated by comparing the extracted meshes against verified reference meshes by a medical expert using a semi-automatic segmentation tool (4D AutoLVQ, GE Vingmed Ultrasound, Norway).

A Doo-Sabin endocardial model controlled by 20 control points was used in the tracking framework. The edge measurements were performed on 528 intensity profiles evenly distributed around the endocardial model. Each profile consisted of 30 samples spaced $1mm$ apart. For the STEP, the normal displacement measurements that were significantly different from their neighbors were discarded as outliers.

In table 1, a Bland-Altman analysis for the surface error measurements is provided. The distribution of the average distance between the tracked and the reference surface points for each edge detector is given. In figure 3,

Surface	ED [mm]	ES [mm]
STEP	3.06 ± 2.03	3.10 ± 2.21
MFMC	2.62 ± 1.74	3.70 ± 2.24
Hybrid	2.50 ± 1.49	3.02 ± 1.88

Table 1. Bland-Altman analysis of the surface measurements: mean error±1.96SD.

Volumetric	EDV [%]	ESV [%]	EF [%]
STEP	-11.4 ± 9.0	2.5 ± 35.2	-6.2 ± 14.0
MFMC	2.9 ± 21.0	23.0 ± 49.1	-8.3 ± 11.7
Hybrid	-2.8 ± 13.9	6.7 ± 36.8	-3.8 ± 11.5

Table 2. Bland-Altman analysis of the volumetric measurements: mean error±1.96SD.

color coded surface error maps are represented for a sample case. In table 2, LV cavity volume errors for ED and ES, and the ejection fraction (EF) errors, all in percentages, are reported.

The tracking framework is implemented in C++, and processed each frame in 7.5ms with STEP, 78ms with MFMC, and 80ms with Hybrid when executed on a 2.80 GHz Intel Core 2 Duo CPU.

4. Discussion and conclusions

In this paper, a graph-cut based edge detection approach MFMC, a hybrid approach combining MFMC and STEP, and their integration into a Kalman filter based tracking framework have been proposed.

Comparative evaluation of the STEP, MFMC and Hybrid showed that the Hybrid leads to improved endocardial surface segmentation results, and hence volumetric measurements. As the accuracy of EF estimation is determined

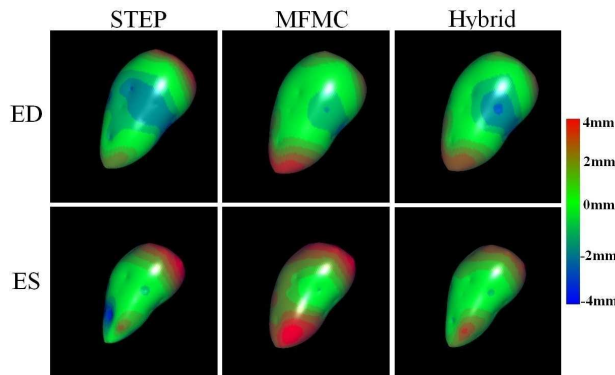


Figure 3. The signed surface errors are represented by using a color coding: 4mm over-estimation is red, 4mm under-estimation is blue, 0mm no-error is light green. ED phase signed errors (the upper row), and ES phase signed errors (the lower row) are shown for a case.

by both ED and ES surface segmentation results, there exists a significant estimation improvement from the closest 6.2% error average produced by STEP to 3.8% using Hybrid.

The tracking framework utilizes a Doo-Sabin surface, which generates the model points evenly distributed around a model. This is ideal for the MFMC implementation proposed in this work. Otherwise, the design of the inter-profile n-link weights should also factor in the varying distances between the profiles.

References

- [1] Blake A, Isard M. Active Contours: The Application of Techniques from Graphics, Vision, Control Theory and Statistics to Visual Tracking of Shapes in Motion. Secaucus, NJ, USA: Springer-Verlag New York, Inc., 1998. ISBN 3540762175.
- [2] Jacob G, Noble JA, Mulet-Parada M, Blake A. Evaluating a robust contour tracker on echocardiographic sequences. Medical Image Analysis 1999;3(1):63 – 75. ISSN 1361-8415.
- [3] Venkatesh S, Owens R. On the classification of image features. Pattern Recogn Lett 1990;11(5):339–349. ISSN 0167-8655.
- [4] Orderud F, Rabben SI. Real-time 3d segmentation of the left ventricle using deformable subdivision surfaces. In CVPR. 2008; .
- [5] Rabben SI, Torp AH, Støylen A, Slørdahl S, Bjørnstad K, Haugen BO, Angelsen B. Semiautomatic contour detection in ultrasound m-mode images. Ultrasound in Medicine Biology 2000;26(2):287 – 296. ISSN 0301-5629.
- [6] Xu N, Ahuja N, Bansal R. Object segmentation using graph cuts based active contours. Comput Vis Image Underst 2007;107(3):210–224. ISSN 1077-3142.
- [7] Slabaugh GG, Unal GB. Graph cuts segmentation using an elliptical shape prior. In ICIP (2). 2005; 1222–1225.
- [8] Greig DM, Porteous BT, Seheult AH. Exact maximum a posteriori estimation for binary images. Journal of the Royal Statistical Society Series B Methodological 1989; 51(2):271–279. ISSN 00359246.
- [9] Goldberg AV, Tarjan RE. A new approach to the maximum-flow problem. J ACM 1988;35(4):921–940. ISSN 0004-5411.
- [10] Papavassiliu T, Kuhl HP, Schroder M, Suselbeck T, Bondarenko O, Bohm CK, Beek A, Hofman MMB, van Rossum AC. Effect of Endocardial Trabeculae on Left Ventricular Measurements and Measurement Reproducibility at Cardiovascular MR Imaging. Radiology 2005;236(1):57–64.

Address for correspondence:

Engin Dikici
 Department of Circulation and Imaging / NTNU
 Olav Kyrres gt. 9; NO-7489 Trondheim
 engin.dikici@ntnu.no